Spoof Surface Plasmon Polariton Leaky-Wave Antennas Using Periodically Loaded Patches Above PEC and AMC Ground Planes

QingLe Zhang, *Student Member, IEEE*, Qingfeng Zhang, *Senior Member, IEEE*, and Yifan Chen, *Senior Member, IEEE*

***Abstract*—This letter proposes two spoof surface plasmon polariton (SSPP) leaky-wave antennas using periodically loaded patches above perfect electric conductor (PEC) and artificial magnetic conductor (AMC) ground planes, respectively. The SSPP leaky-wave antenna is based on an SSPP transmission line, along which circular patches are periodically loaded on both sides to provide an additional momentum for phase matching with the radiated waves in the air. The PEC and AMC ground planes underneath the antenna reflect the radiated waves into the upward space, leading to an enhanced radiation gain. Both PEC- and AMC-grounded antenna prototypes are fabricated and measured in comparison with the one without any ground plane. The experimental results show that the PEC and AMC ground planes increase the radiation gain by approximately 3 dB within the operational frequency range 4.5–6.5 GHz. It also demonstrates that the AMC-grounded leaky-wave antenna, with a thickness of $0.08\lambda_0$ at 6 GHz, features more compact profile than the PEC-grounded one (with a thickness of $0.3\lambda_0$ at 6 GHz).**

***Index Terms*—Artificial magnetic conductor (AMC), perfect electric conductor (PEC), leaky-wave antenna, spoof surface plasmon polaritons (SSPP).**

I. Introduction

COMPLEX waves are important electromagnetic modes and have been extensively explored in open structures [1]–[3]. Surface wave, supported by the interface of two mediums, is a guided complex wave whose fields intensity exponentially decay away from the interface. The study of surface waves has a long history in microwave community, dating back at least to 1900s by Sommerfeld [4] and Zenneck [5]. Spoof surface plasmon polaritons (SSPP) [6], although proposed recently and inspired by surface plasmons in optics, belong to the general category of complex waves, and share almost the same properties as the surface waves supported by patterned metals [2] and a corrugated Goubau line [7].

Recently, SSPP has attracted much attention due to its highly confined field in a subwavelength scale and potential applications to ultrathin and flexible circuits [8]. Basically, SSPP only supports a slow-wave surface mode that does not radiate. To achieve the radiation, Xu *et al.* periodically modulate the SSPP metallic strips [9]. Gu *et al.* proposed a leaky-wave antenna using nonuniformly modulated plasmonic waveguide [10], and employed an asymmetrical profile to get a high-efficiency broadside radiation. In [11], a circular patch array fed by a planar SSPP transmission line was presented. In [12], a single-layer leaky-wave antenna without loading terminations was reported. Meanwhile, surface-wave guiding and radiating structures based on planar Goubau lines [7], [13], [14] were explored in parallel. Generally, SSPP exhibits better field confinement capability than the Goubau line, although both of them operate in similar principles. So, we focus on SSPP in this letter.

Since SSPP is a single-conductor line without any ground plane, most SSPP leaky-wave antennas exhibit omnidirectional H-plane radiations due to the quasicircular symmetrical profiles. This is not preferred in some applications that require directional beams. In this letter, we propose an SSPP leaky-wave antenna using periodically loaded circular patches incorporating with either a perfect electric conductor (PEC) or an artificial magnetic conductor (AMC) ground plane underneath the antenna to achieve directional beams in the H plane. It shows that both ground planes improve the radiation gain by approximately 3 dB. The optimum distance of the PEC ground plane is $0.3\lambda_0$ at 6 GHz. In contrast, the AMC ground plane gets much closer to the radiator, around $0.08\lambda_0$ at 6 GHz. Therefore, the AMC-grounded SSPP leaky-wave antenna performs better in low-profile applications.

II. SSPP Transmission Line

The configuration of the SSPP transmission line is shown in Fig. 1(a). It is fabricated on a 1 mm thick F4B substrate (with $\epsilon_r = 2.65$ and $\tan\delta = 0.003$). Since the SSPP transmission line is a single-conductor line not compatible with the SMA connector, a smooth transition into $50\,\Omega$ coplanar waveguide (CPW) is designed for both impedance transformation and mode conversion. The overall width and length of the SSPP transmission line

Manuscript received June 13, 2017; accepted September 27, 2017. Date of publication October 2, 2017; date of current version November 8, 2017. This work was supported in part by the Guangdong NSF for DYS (2015A030306032), in part by NSFC (61401191), in part by Guangdong STD funds (2016 TQ03X839), in part by Shenzhen STIC funds (KQJSCX20160226193445, JCYJ20150331101823678, KQCX2015 033110182368, JCYJ2016030111 3918121, JSGG20160427105120572), and in part by Shenzhen DRC under Grant [2015]944. *(Corresponding author: Qingfeng Zhang.)*

Q. Zhang and Q. L. Zhang are with the Southern University of Science and Technology, Shenzhen 518055, China (e-mail: zhang.qf@sustc.edu.cn; qingle.zhang@hotmail.com).

Y. Chen is with the University of Waikato, Hamilton 3216, New Zealand (e-mail: chenyf@sustc.edu.cn).

Color versions of one or more of the figures in this letter are available online at http://ieeexplore.ieee.org.

Digital Object Identifier 10.1109/LAWP.2017.2758368

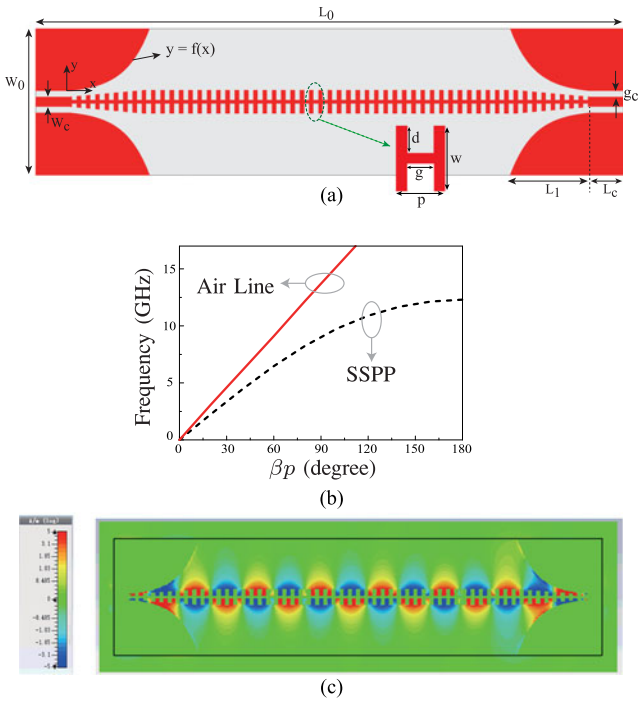

Fig. 1. (a) Geometry configuration of the SSPP transmission line without ground plane. (b) Dispersion curve of the SSPP unit cell. (c) Calculated magnetic field H_z distribution at 6 GHz.

including the CPW transition are $w_0 = 70$ mm and $L_0 = 328$ mm, respectively. For the CPW transmission line at the ports, the strip width, gap size, and length are chosen as $w_c = 2.3$ mm, $g_c = 0.2$ mm, and $L_c = 10$ mm, respectively. To accommodate the single-conductor SSPP line, the CPW ground planes gradually fade away in an exponential function, $y = f(x) = e^{\alpha x} - 1$, where $\alpha = \ln(w_0/2 - w_c/2 - g_c + 1)/L_1$ and $L_1 = 47.5$ mm. The gradually tapered ground plane reduces the equivalent capacitance, and hence, increases the characteristics impedance for matching with the SSPP line. In fact, the SSPP transmission line can also be regarded as a multi-conductor line with ground planes placed at an infinite distance. Thus, this tapered ground plane is a natural transition for SSPP line. Besides, the exponentially tapered ground plane also produces a longitudinal electric field, which provides a smooth TEM-to-TM mode conversion.

The SSPP transmission line employs an H-shape corrugated strip, whose parameters are $p = 5.5$ mm, $w = 9.5$ mm, $d = 4$ mm, and $g = 3$ mm. This H-shape unit cell is analyzed by the Eigen-mode solver of CST Microwave Studio, and the computed dispersion curve is shown Fig. 1(b). Note that the supported mode is always below the air line [shown as the red solid line in Fig. 1(b)], and hence, it is a bounded slow-wave mode. The dispersion curve gradually bends away from the air line when the operational frequency increases up to the cutoff frequency at 12.3 GHz. Since the momentum of this mode is always smaller than that of the wave in the air, the field does not radiate into the air, and hence, is well confined along the line. Fig. 1(c) displays the computed magnetic field on the substrate at 6 GHz. One clearly observes a well-confined surface mode propagating along the SSPP transmission line. Also, the field is alternating

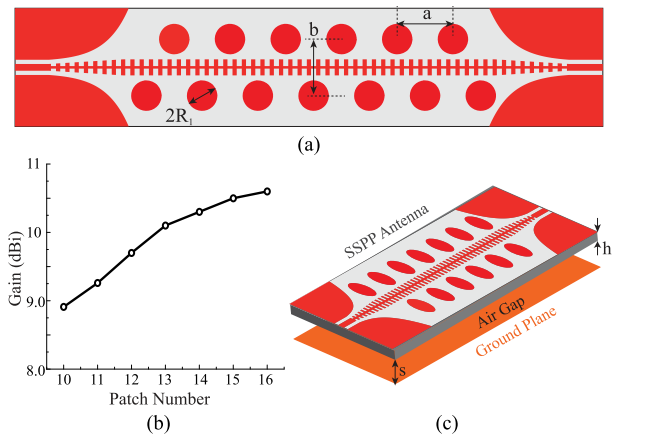

Fig. 2. (a) Configuration of the patch-loaded SSPP leaky-wave antenna. (b) Gain response at 6 GHz versus patch number. (c) Ground plane underneath the SSPP leaky-wave antenna.

between the two sides of the H-shape line. This allows one to load patches on both sides of the SSPP line to achieve leaky-wave radiations, which will be introduced in the forthcoming section.

III. SSPP Leaky-Wave Antenna

As illustrated in Fig. 1(b) and (c), the SSPP transmission line supports a slow-wave surface mode, which does not radiate due to lack of enough wave momentum. To achieve radiation, it requires an additional momentum, which may be realized either by periodically modulating the profile [9], or by periodically loading circular patches along the SSPP line [11]. Here, we employ patch loading on both sides of the SSPP line, as shown in Fig. 2(a). In order to excite all the patches in phase at 6 GHz, one may align all the patches using the red spots of Fig. 1(c). Therefore, all the patches are placed on both sides of the SSPP line in an alternating fashion, with a separation distance of half wavelength. According to the dispersion curve in Fig. 1(b), the SSPP guided wavelength is $\lambda_g = 2\pi/\beta = 36$ mm at 6 GHz. So, the patch loading period should be the same as the guided wavelength, i.e., $a = \lambda_g = 36$ mm. One should note that the loaded patches will slightly change the field distribution, and hence, the guided wavelength of the SSPP line because each patch brings in an extra resistance (due to radiation) and reactance. So, the resultant excitation may not be exactly in phase at 6 GHz. The patch radius R_1 and the distance from the SSPP line $b/2$ are used to control the coupling level, and hence, the radiated power of each element. In our design, we choose $R_1 = \lambda_g/4 = 9$ mm and $b = 28.5$ mm. Once the leakage from each element is fixed by R_1 and b, one may choose an optimum patch number to efficiently radiate most of the power. Fig. 2(b) shows the maximum gain at 6 GHz versus the patch number. When the patch number is less than 13, the gain increases quickly as the number increases. However, it increases slowly after 13. It turns out that most of the power has been radiated out by 13 patches and the additional patches do not reward too much at the expense of an increased aperture. Therefore, one may choose 13 pathes in this design. Compared with the single-side loading structure in [11], this patch loading on both sides of the line greatly enhances the efficiency of space utilization.

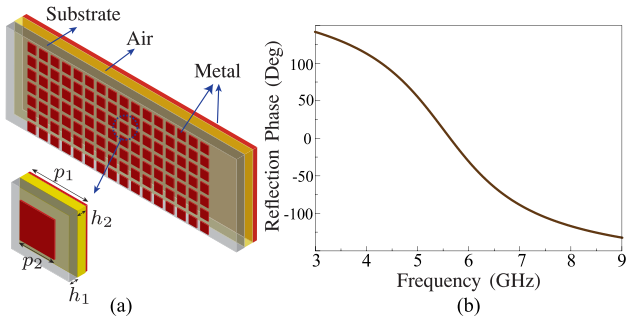

Fig. 3. (a) Configuration of the AMC ground plane. (b) Reflection phase of the AMC plane under perpendicular incidence.

In addition to patch loading on both sides of the SSPP line, the proposed leaky-wave antenna also employs a ground plane underneath it, as shown in Fig. 2(c). The ground plane reflects the waves into the upper space, and hence, increases the radiation gain. We explore both PEC and AMC ground planes in this research. The distance between the ground plane and the antenna s should be optimized for different cases. The ideal distance for a PEC ground plane should be around a quarter of the space wavelength so that the reflected wave are in phase with the directly radiated wave. In this design, the optimum distance for the PEC ground plane is $s = 0.3\lambda_0 = 15$ mm, where λ_0 is the space wavelength at 6 GHz. In contrast, the AMC ground plane can be placed much closer to the antenna. Fig. 3(a) depicts the geometry of the AMC ground, which is formed by periodic square patches printed on an F4B substrate with an air-gapped metal plane underneath it. The thickness of the substrate h_1, the air gap h_2, the patch size p_2, and the patch period p_1 are optimized to maximize the operational bandwidth. The optimum parameters are $h_1 = 2$ mm, $h_2 = 2$ mm, $p_2 = 8.3$ mm, and $p_1 = 10$ mm. Fig. 3(b) shows the reflection phase under perpendicular incidence. Note that the operational frequency range is 4.45–7.04 GHz, within which the reflection phase stays between $+90^\circ$ and -90°. This multilayer AMC structure exhibits broader bandwidth than the typical single-layer configuration in [15]. When placing this AMC underneath the SSPP leaky-wave antenna, the optimum distance $s = 4$ mm is only 26.7% of the PEC case. Even counting in the AMC thickness, the overall distance ($h_1 + h_2 + s = 8$ mm) is still 53% of the PEC case. Therefore, AMC-grounded SSPP leaky-wave antenna features more compact profile than the PEC-grounded one.

IV. Experimental Validation

To experimentally verify the performance of the PEC-grounded and AMC-grounded SSPP leaky-wave antennas, they are fabricated and measured in comparison with the one without any ground plane. In Fig. 4(a), the top figure shows the fabricated prototype of the SSPP leaky-wave antenna with loaded circular patches on both sides of the SSPP line, and the bottom figure displays the fabricated prototype of the AMC ground (in top view). Since the PEC ground is purely metals, its fabricated prototype is not shown here. Fig. 4(b) illustrates the assembly photograph of both PEC-grounded and AMC-grounded SSPP leaky-wave antennas. Different layers are piled up with finely tuned air gaps. Plastic screws are placed at four edge corners to

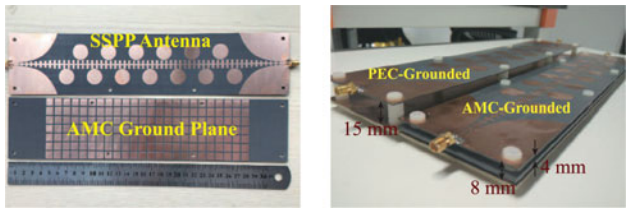

Fig. 4. Photograph of the fabricated prototypes: (a) SSPP leaky-wave antenna and AMC ground plane; and (b) comparison of PEC-grounded antenna and AMC-grounded antenna.

fix the distance between layers. One clearly observes that AMC-grounded SSPP leaky-wave antenna is much thinner than the PEC-grounded one. All the fabricated prototypes are measured in an Agilent vector network analyzer E5071C for reflection responses and an Anechoic Chamber for radiation patterns and gains.

One first compares the SSPP leaky-wave antennas with and without a PEC ground plane. Fig. 5(a) shows the simulated and measured reflection responses of both cases. The measured responses agree well with the simulated ones within the whole measured frequency range from 3 to 7 GHz. Also, the reflections of both SSPP leaky-wave antennas with and without PEC ground plane are below -10 dB within the frequency band 4–7 GHz (with a relative bandwidth of 54.5%). It turns out that the PEC ground plane does not affect the impedance matching of the SSPP leaky-wave antenna. This is possibly attributed to the highly confined field of the SSPP transmission line and its relatively large separation (around $0.3\lambda_0$) from the PEC ground. Although the PEC ground plane does not affect the reflection response, it increases the radiation gain by reflecting the downward waves into the upper space. Fig. 5(b) compares the radiation gains of SSPP leaky-wave antennas with and without a PEC ground plane. The PEC ground plane increases the radiation gain by almost 3 dB within the frequency range 4–5.5 GHz, inspite of a smaller increment after 5.5 GHz. The measured and simulated total efficiencies for both cases are around 80% within 4–5.5 GHz. Furthermore, the measured responses agree well with the simulated ones for both cases. The maximum measured radiation gain is around 14.1 dBi for the PEC-grounded SSPP leaky-wave antenna. Fig. 5(c) shows the simulated and measured xz-plane radiation patterns of the PEC-grounded antenna at different frequencies. The measured beam, in a good agreement with the simulated one, continuously scans from -32° to 13° as the frequency increases from 4.5 to 6.5 GHz.

For the AMC-grounded SSPP leak-wave antenna, its simulated and measured reflection responses are shown in Fig. 6(a). Similar to the PEC-grounded case, the measured reflection response, in good agreement with the simulated one, is below -10 dB within the frequency band 4–7 GHz. Therefore, the AMC ground does not affect the impedance matching as well although it stays much closer to the SSPP leaky-wave antenna. Fig. 6(b) compares the radiation gains of the SSPP leaky-wave antennas with and without an AMC ground plane. The AMC ground plane also increases the radiation gain by almost 3 dB within the frequency range 4–5.5 GHz, inspite of a degradation after 5.5 GHz. The measured and simulated total efficiencies

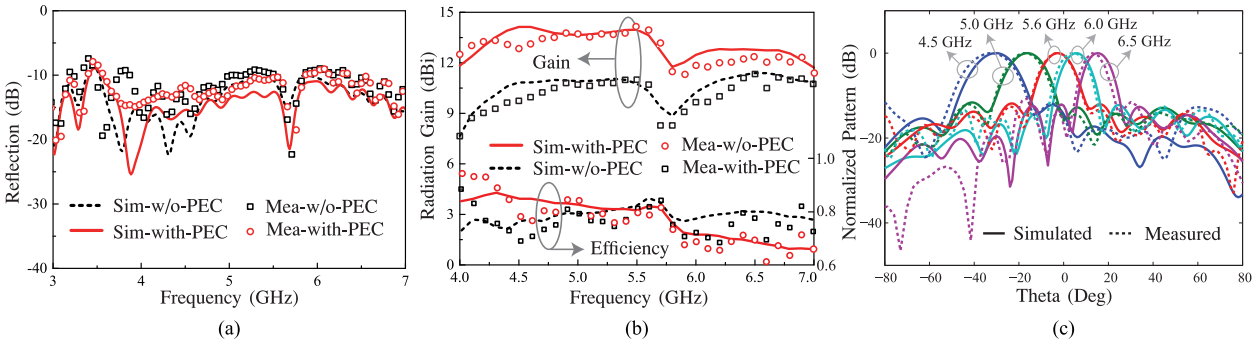

Fig. 5. Simulated and measured (a) reflection responses and (b) radiation gain and total efficiency of the SSPP antenna with and without PEC grounds; (c) simulated and measured radiation patterns of PEC-grounded SSPP antenna at different frequencies (radiation patterns are normalized to the maximum values at individual frequencies).

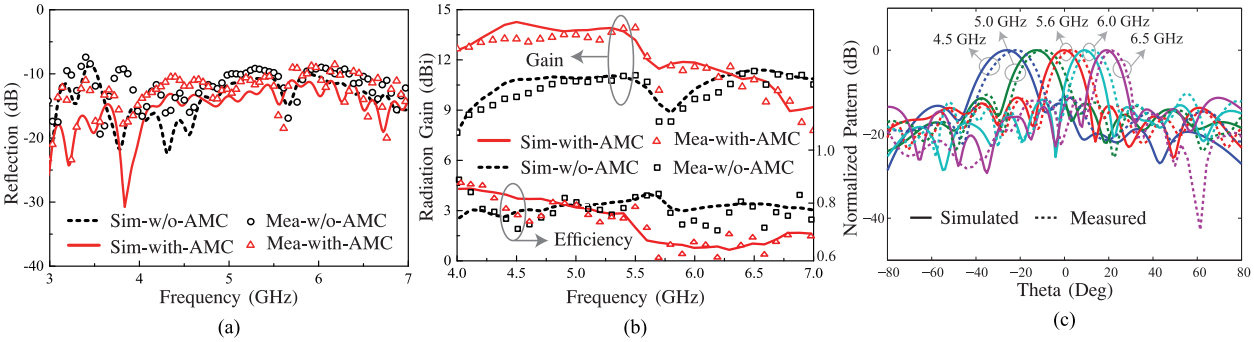

Fig. 6. Simulated and measured (a) reflection responses and (b) radiation gain and total efficiency of the SSPP antenna with and without AMC grounds; (c) simulated and measured radiation patterns of AMC-grounded SSPP antenna at different frequencies (radiation patterns are normalized to the maximum values at individual frequencies).

for both cases are all round 80% within 4–5.5 GHz, and the maximum measured gain is around 13.9 dBi. Fig. 6(c) shows the simulated and measured xz-plane radiation patterns of the AMC-grounded antenna at different frequencies. The measured beam, continuously scanning from -22° to 21° as the frequency increasing from 4.5 to 6.5 GHz, exhibit a constant shift compared with the simulated result. This slight shift is possibly attributed to the tolerances mainly contributed by the two air gaps between layers, which is brought by manual assembly.

V. Conclusion

SSPP leaky-wave antennas using loaded patches above a PEC and an AMC ground plane, respectively, have been introduced. The results reveal that both ground planes increase the radiation gain by almost 3 dB. The AMC-grounded antenna features a more compact profile than the PEC-grounded one.

Acknowledgment

This work was measured at the City University of Hong Kong, Hong Kong.

References

[1] T. Tamir and A. A. Oliner, "Guided complex waves. Part 1: Fields at an interface," *Proc. Inst. Electr. Eng.*, vol. 110, no. 2, pp. 310–324, Feb. 1963.

[2] F. J. Zucker, "Surface- and leaky-wave antennas," in *Antenna Engineering Handbook*. New York, NY, USA: McGraw-Hill, 1961.

[3] A. Ishimaru, *Electromagnetic Wave Propagation, Radiation, and Scattering*. Englewood Cliffs, NJ, USA: Prentice-Hall, 1991.

[4] A. Sommerfeld, "Propagation of waves in wireless telegraphy," *Ann. Phys*, vol. 28, no. 3, pp. 665–736, 1909.

[5] J. Zenneck, "Propagation of plane EM waves along a plane conducting surface," *Ann. Phys.*, vol. 23, no. 1, pp. 846–866, May 1907.

[6] J. B. Pendry, L. Martin-Moreno, and F. J. Garcia-Vidal, "Mimicking surface plasmons with structured surfaces," *Science*, vol. 305, no. 5685, pp. 847–848, 2004.

[7] S. Laurette, A. Treizebre, and B. Bocquet, "Corrugated Goubau lines to slow down and confine THz waves," *IEEE Trans. THz Sci. Technol.*, vol. 2, no. 3, pp. 340–344, May 2012.

[8] X. Shen, T. J. Cui, D. Martin-Cano, and F. J. Garcia-Vidal, "Conformal surface plasmons propagating on ultrathin and flexible films," *Proc. Nat. Acad. Sci.*, vol. 110, no. 1, pp. 40–45, 2013.

[9] J. J. Xu, H. C. Zhang, Q. Zhang, and T. J. Cui, "Efficient conversion of surface-plasmon-like modes to spatial radiated modes," *Appl. Phys. Lett.*, vol. 106, Dec. 2015, Art. no. 021102.

[10] S. K. Gu, H. F. Ma, B. G. Cai, and T. J. Cui, "Continuous leaky-wave scanning using periodically modulated spoof plasmonic waveguide," *Sci. Rep.*, vol. 6, Jul. 2016, Art. no. 29600.

[11] J. Y. Yin *et al.*, "Frequency-controlled broad-angle beam scanning of patch array fed by spoof surface plasmon polaritons," *IEEE Trans. Antennas Propag.*, vol. 64, no. 12, pp. 5181–5189, Dec. 2016.

[12] A. Kianinejad, Z. N. Chen, and C.-W. Qiu, "A single-layered spoof plasmon leaky wave antenna with consistent gain," *IEEE Trans. Antennas Propagation*, vol. 65, no. 2, pp. 681–687, Feb. 2017.

[13] A. K. Horestani *et al.*, "Metamaterial-inspired bandpass filters for terahertz surface waves on Goubau lines," *IEEE Trans. THz Sci. Technol.*, vol. 3, no. 6, pp. 851–858, Nov. 2013.

[14] D. Snchez-Escuderos, M. Ferrando-Bataller, J. I. Herranz, and M. Cabedo-Fabrs, "Periodic leaky-wave antenna on planar Goubau line at millimeter-wave frequencies," *IEEE Antennas Wireless Propag. Lett.*, vol. 12, pp. 1006–1009, Aug. 2013.

[15] D. Sievenpiper, L. Zhang, R. F. Broas, N. G. Alexopolous, and E. Yablonovitch, "High-impedance electromagnetic surfaces with a forbidden frequency band," *IEEE Trans. Microw. Theory Techn.*, vol. 47, no. 11, pp. 2059–2074, Nov. 1999.